

1 Mechanistic numerical modeling of solute uptake
2 by plant roots

3 Andre Herman Freire Bezerra * Quirijn de Jong van Lier
4 Sjoerd E.A.T.M van der Zee Peter de Willingen

5 January, 2016

*Bezerra, A.H.F. and Q. de Jong van Lier, Exact Sciences Dep., ESALQ–Univ. of São Paulo, 13418-900 Piracicaba (SP), Brazil; S.E.A.T.M. van der Zee and P. Willingen, Dep. of Environmental Sciences, Wageningen Univ., Droevendaalsesteeg 4, 6708 PB Wageningen, the Netherlands.

6 Core ideas

- 7 • idea 1
- 8 • idea 2
- 9 • idea 3
- 10 • optional idea 4
- 11 • optional idea 5

12 Abstract

13 A modification in an existing water uptake and solute transport numerical model
14 was implemented in order to allow the model to simulate solute uptake by the
15 roots. The convection-dispersion equation (CDE) was solved numerically, using
16 a complete implicit scheme, considering a transient state for water and solute
17 fluxes and a soil solute concentration dependent boundary for the uptake at the
18 root surface, based on the Michaelis-Menten (MM) equation. Additionally, a
19 linear approximation was developed for the MM equation such that the CDE
20 has a linear and a non-linear solution. A radial geometry was assumed, consid-
21 ering a single root with its surface acting as the uptake boundary and the outer
22 boundary being the half distance between neighboring roots, a function of root
23 density. The proposed solute transport model includes active and passive so-
24 lute uptake and predicts solute concentration as a function of time and distance
25 from the root surface. It also estimates the relative transpiration of the plant,
26 on its turn directly affecting water and solute uptake and related to water and
27 osmotic stress status of the plant. Performed simulations show that the linear
28 and non-linear solutions result in significantly different solute uptake predic-
29 tions when the soil solute concentration is below a limiting value (C_{lim}). This
30 reduction in uptake at low concentrations may result in a further reduction in
31 the relative transpiration. The contributions of active and passive uptake vary
32 with parameters related to the ion species, the plant, the atmosphere and the
33 soil hydraulic properties. The model showed a good agreement with an ana-
34 lytical model that uses a linear concentration dependent equation as boundary
35 condition for uptake at the root surface. The advantage of the numerical model
36 is it allows simulation of transient solute and water uptake and, therefore, can
37 be used in a wider range of situations. Simulation with different scenarios and
38 comparison with experimental results are needed to verify model performance
39 and possibly suggest improvements.

40 Text

41 Crop growth is directly related to plant transpiration, and the closer the cumu-
42 lative transpiration over a growing season is to its potential value, the higher
43 will be the crop yield. Any stress occurring during crop development results in
44 stomata closure and transpiration reduction, affecting productivity. Therefore,
45 knowing how plants respond to abiotic stresses like those related to water and
46 salt, and predicting and quantifying them, is important not only to improve

the understanding of plant-soil interactions, but also to propose better crop management practices. The interpretation of experimental data to analyze the combined water and salt stress on transpiration and yield has been shown to be difficult due to the great range of possible interactions between the factors determining the behavior of the soil-plant-atmosphere (SPA) system. Modeling has been shown to be an elucidative manner to analyze the involved processes and mechanisms, providing insight in the interaction of water and salt stress.

Analytical models describing transport of nutrients in soil towards plant roots usually consider steady state conditions with respect to water flow to deal with the high non-linearity of soil hydraulic functions. Several simplifications (assumptions) are needed regarding the uptake of solutes by the roots, most of them also imposed by the non-linearity of the influx rate function. Consequently, although analytical models describe the processes involved in transport and uptake of solutes, they are only capable of simulating water and solute flow just for specific boundary conditions. Therefore, applying these models in situations that do not exactly correspond to their boundary condition may lead to a rough approximation but may also result in erroneous predictions. Many of the available analytical solutions include special math functions (Bessels, Airys or infinite series, for example) that need, at some point, numerical algorithms to compute results. For the case of the convection-diffusion equation, even the fully analytical solutions are restricted by numerical procedures, although with computationally efficient and reliable results.

As a substitute to analytical solutions, numerical modeling allows more flexibility when dealing with non-linear equations, being an alternative to better cope with diverse boundary conditions. The functions can be solved considering transient conditions for water and solute flow but with some pullbacks regarding numerical stability and more processing to perform calculations. In general, numerical models use empirical functions that relate osmotic stress to some electric conductivity of the soil solution. The parameters of these empirical models depend on soil, plant and atmospheric conditions in a range covered by the experiments used to generate data for model calibration. Using these models out of the measured range is not recommended and, in these cases, a new parameter calibration should be done. Physical/mechanistic models for the solute transport equations describe the involved processes in a wider range of situations since it is less dependent on experimental data, giving more reliable results.

In this study, we develop a mechanistic based numerical scheme to solve the convection-dispersion equation for radial root solute extraction. The model uses the water uptake scheme from De Jong van Lier et al. (2006). Assuming a boundary condition at root surface of concentration dependent solute uptake, the solution for the CDE considers transient flow of water and solute, as well as root competition. The model allows prediction of active and passive contributions to the solute uptake, which can be used to separate ionic and osmotic stresses by considering solute concentration inside the plant.

91 MATERIAL AND METHODS

92 Hydraulic Properties and Soil

93 Water uptake was analyzed using hydraulic data for three topsoils from the
 94 Dutch Staring series (Wösten et al., 2001) as listed in Table 1. The Van
 95 Genuchten (1980) equation system was used to describe K - θ - h relations for
 96 these soils:

$$\theta(h) = \theta_r + \frac{\theta_s - \theta_r}{[1 + |\alpha h|^n]^{1-(1/n)}} \quad (1)$$

$$K(\theta) = K_s \Theta^\lambda [1 - (1 - \Theta^{n/(n-1)})^{(1-(1/n))}]^2 \quad (2)$$

97 where θ ($\text{m}^3 \text{m}^{-3}$) is the water content, K (m s^{-1}) and K_s (m s^{-1}) are respec-
 98 tively the hydraulic conductivity and the saturated hydraulic conductivity, h
 99 is the pressure head (m), Θ (-) is the effective saturation defined by $\frac{(\theta - \theta_r)}{(\theta_s - \theta_r)}$;
 100 θ_s ($\text{m}^3 \text{m}^{-3}$) and θ_r ($\text{m}^3 \text{m}^{-3}$) are the saturated and residual water contents,
 101 respectively; and α (m^{-1}), λ (-) and n (-) are empirical parameters.

Table 1: Soil hydraulic parameters used in simulations

Staring soil ID	Textural class	Reference in this paper	θ_r $\text{m}^3 \text{m}^{-3}$	θ_s $\text{m}^3 \text{m}^{-3}$	α m^{-1}	λ -	n -	K_s m d^{-1}
B3	Loamy sand	Sand	0.02	0.46	1.44	-0.215	1.534	0.1542
B11	Heavy clay	Clay	0.01	0.59	1.95	-5.901	1.109	0.0453
B13	Sandy loam	Loam	0.01	0.42	0.84	-1.497	1.441	0.1298

102 Model Description

103 Microscopic root uptake models consider a single cylindrical root of radius r_0 (m)
 104 with an extraction zone being represented by a concentric cylinder of radius r_m
 105 (m) that bounds the half-distance between roots. The height of both cylinders
 106 is z (m) and represents the rooted soil depth. The basic assumptions of this
 107 type of model is that the root density does not change with depth and there is
 108 no difference in intensity of extraction along the root surface. Water and solute
 109 flows are axis-symmetric.

110 It is common to report root length density R (m m^{-3}) and r_0 . These are
 111 related to r_m and root length L (m) by the following equations:

$$r_m = \frac{1}{\sqrt{\pi R}} \quad (3)$$

$$L = \frac{A_p z}{\pi r_m^2} \quad (4)$$

112 where A_p (m^2) is the soil surface area occupied by the plant. For the case
 113 that there is no available data from literature, one can obtain the value of L
 114 from relatively simple measurements of root and soil characteristics as soil mass
 115 (m_s , kg) and density (d_s , kg m^{-3}), and root average radius (\bar{r}_0 , m) and R by

$$R = \frac{1}{\pi r_m^2}. \quad (5)$$

The geometry of the soil-root system considers an uniformly distributed parallel cylindrical root of radius r_0 and length z . To each root, a concentric cylinder of radius r_m and length z can be assigned to represent its extraction volume (Figure 1).

The discretization needed for the numerical solution was performed at the single root scale. As the extraction properties of the root are considered uniform along its length, and assuming no vertical differences in root density and fluxes, the cylinder can be represented by its cross-section, a circle. The area of this circle, representing the extraction region, was subdivided into n circular segments of variable size Δr (m), small near the root and increasing with distance, according to the equation De Jong van Lier et al. (2009):

$$\Delta r = \Delta r_{min} + (\Delta r_{max} - \Delta r_{min}) \left(\frac{r - r_0}{r_m - r_0} \right)^S \quad (6)$$

where the subscripts in Δr indicate the minimum and maximum segment sizes defined by the user, and S gives the rate at which the segment size increases. The parameter r_0 (m) represents the root radius, and r_m (m) is the radius of the root extraction zone, equal to the half-distance between roots, which relates to the root density R (m m⁻³) according to Equation 3. This variable size discretization has the advantage to result in smaller segments in regions that need more detail in the calculations (near the root soil interface) due to the greater variation of expected fluxes. Figure 2 shows a schematic representation of the discretization as projected by Equation 6.

A fully implicit numerical treatment was given to the water and solute balance equations ?? and ?. The Richards equation ?? for one-dimensional axis-symmetric flow can be written as

$$\frac{\partial \theta}{\partial t} = \frac{\partial \theta}{\partial H} \frac{\partial H}{\partial t} = C_w(H) \frac{\partial H}{\partial t} = \frac{1}{r} \frac{\partial}{\partial r} \left(r K(h) \frac{\partial H}{\partial r} \right) \quad (7)$$

where the total hydraulic head (H) is the sum of pressure (h) and osmotic (h_π) heads and C_w (m⁻¹) is the differential water capacity $\frac{\partial H}{\partial \theta}$. Relations between K , θ and h are described by the Van Genuchten (1980) equation system (Equations 1 and 2). Analogous to Van Dam and Feddes (2000), Equation 7 can be solved using an implicit scheme of finite differences with the Picard iterative process:

$$C_{w_i}^{j+1,p-1} (H_i^{j+1,p} - H_i^{j+1,p-1}) + \theta_i^{j+1,p-1} - \theta_i^j = \frac{t^{j+1} - t^j}{r_i \Delta r_i} \times \left[r_{i-1/2} K_{i-1/2}^j \frac{H_{i-1}^{j+1,p} - H_i^{j+1,p}}{r_i - r_{i-1}} - r_{i+1/2} K_{i+1/2}^j \frac{H_i^{j+1,p} - H_{i+1}^{j+1,p}}{r_{i+1} - r_i} \right] \quad (8)$$

where i ($1 \leq i \leq n$) refers to the segment number, j is the time step and p the iteration level. The Picard's method is used to reduce inaccuracies in the implicit numerical solution for the h -based Equation 7 Celia et al. (1990).

148 The solution for Equation 8 results in prediction of pressure head in soil as
 149 a function of time and distance from the root surface. The boundary conditions
 150 considered relate the flux density entering the root to the transpiration rate for
 151 the inner segment; and considers zero flux for the outer segment:

$$K(h) \frac{\partial h}{\partial r} = q = 0, \quad r = r_m \quad (9)$$

$$K(h) \frac{\partial h}{\partial r} = q_0 = \frac{T_p}{2\pi r_0 R z}, \quad r = r_0 \quad (10)$$

152 The computer algorithm that solves the Equation 8 and applies boundary
 153 conditions 9 and 10 can be found in Appendix ??.

154 The convection-dispersion equation ?? for one-dimensional axis-symmetric
 155 flow can be written as

$$r \frac{\partial(\theta C)}{\partial t} = -\frac{\partial}{\partial r} \left(r q C \right) + \frac{\partial}{\partial r} \left(r D \frac{\partial C}{\partial r} \right). \quad (11)$$

156 with initial condition corresponding to constant solute concentration (C_{ini}) in
 157 all segments:

$$C = C_{ini}, \quad t = 0, \quad r = r_i, \quad 1 \leq i \leq n. \quad (12)$$

158 Both boundary conditions are of the flux type, according to

$$-D(\theta) \frac{\partial C}{\partial r} \Big|_{r=r_i} + qC = F, \quad t > 0, \quad r_i = \{r_0, r_m\}. \quad (13)$$

159 From the assumed geometry (Figure 2) it follows that the boundary condi-
 160 tion at the outer segment corresponds to zero solute flux (q_s):

$$F = 0, \quad r = r_m. \quad (14)$$

The rate of solute uptake by plant roots can be described by the MM equation, as seen in Chapter ?. The uptake shape function $\alpha(C)$ can be supposed to follow the concentration dependent MM kinetics, and considering k equal to I_m leads to:

$$\alpha(C) = \frac{C}{K_m + C} \Rightarrow F = \frac{C}{K_m + C} I_m \quad (15)$$

161 where I_m is the maximum uptake rate, C is the solute concentration in soil so-
 162 lution and K_m the Michaelis-Menten constant. I_m can be found experimentally
 163 and K_m is to be calibrated as the concentration at which I_m assumes half of its
 164 value, being interpreted as the affinity of the plant for the solute.

165 The boundary condition for solute transport at the root surface (r_0) repre-
 166 sents the concentration dependent solute uptake, described by the MM equation
 167 15, with the following assumptions:

- 168 • Solute uptake by mass flow of water is only controlled by the transpiration
 169 flow, a convective flow that is considered to be passive;
- 170 • Plant regulated active uptake corresponds to diffusion;

- 171 • Plant demand is equal to the I_m parameter from the MM equation;
- 172 • At a soil solution concentration value C_{lim} , the solute flux limits the up-
- 173 take.

174 We assume that the plant demand for solute is constant in time. The uptake,
 175 however, can be higher or lower than the demand, depending on the concen-
 176 tration in the soil solution at the root surface (Figure 3). If the concentration
 177 is bellow a certain limiting value (C_{lim}), the uptake is limited by the solute
 178 flux, *i.e.* solute flux can not attend plant demand even with potential values of
 179 active uptake. Additionally, solute uptake by mass flow of water can be higher
 180 than the plant demand in situations of high transpiration rate and/or for high
 181 soil water content. In these cases, we assume that active uptake is zero and
 182 all uptake occurs by the passive process. A concentration C_2 (mol) for this
 183 situation is calculated. When the concentration is between C_{lim} and C_2 , the
 184 uptake is equal to the plant demand as a result of the sum of active and passive
 185 contributions to the uptake. Assumption 1 states that passive uptake is not
 186 controlled by any physiological plant mechanisms and, in order to optimize the
 187 use of metabolic energy, active uptake is regulated in such way that it works as a
 188 complementary mechanism of extraction to achieve plant demand (Assumption
 189 2). This results in a lower active uptake contribution than that of its potential
 190 value. However, the effect of the solute concentration inside the plant on solute
 191 uptake and plant demand is not considered in the model. Consequently, a sce-
 192 nario for which the demand is reduced due to an excess of solute concentration
 193 in the plant is not considered. This might, in certain situations, lead to an
 194 overestimated prediction of uptake.

A piecewise non-linear uptake function that considers these explicit bound-
 ary conditions was formulated as:

$$F = \begin{cases} \frac{I_m C_0}{K_m + C_0} + q_0 C_0, & \text{if } C_0 < C_{lim} \\ I_m, & \text{if } C_{lim} \leq C_0 \leq C_2 \\ q_0 C_0, & \text{if } C_0 > C_2 \end{cases} \quad (16)$$

$$I_m, \quad \text{if } C_{lim} \leq C_0 \leq C_2 \quad (17)$$

$$q_0 C_0, \quad \text{if } C_0 > C_2 \quad (18)$$

with C_{lim} determined by the positive root of

$$C_{lim} = -\frac{K_m \pm (K_m^2 + 4I_m K_m / q_0)^{1/2}}{2}, \quad (19)$$

and C_2 by

$$C_2 = \frac{I_m}{q_0}. \quad (20)$$

The non-linear part of the uptake function resides in Equation 16. As im-
 plicit numerical implementations of non-linear functions may result in solutions
 with stability issues, a linearization of Equation 16 was made, resulting in:

$$F = (\alpha + q_0) C_0, \quad \text{if } C_0 < C_{lim} \quad (21)$$

195 where α (m s^{-1}) and q_0 (m s^{-1}) are the active and passive contributions for the
 196 solute uptake slope ($\alpha + q_0$). This linearization is very similar to the one proposed
 197 by Tinker and Nye (2000), but does not consider the solute concentration inside
 198 the plant. The derivation of Equations 19 to 21 is shown in Appendix ??.

199 Finally, the boundary condition at the inner segment refers to the concentra-
 200 tion dependent solute flux at the root surface (F , mol m⁻² d⁻¹) in agreement to
 201 Equation 21 for the non-linear and linear case, respectively. The uptake of
 202 each root equals $-F/R$ (mol d⁻¹, the negative sign indicating solute depletion),
 203 thus, the condition at the root surface is described by:

$$-D(\theta)\frac{\partial C}{\partial r} + q_0 C_0 = q_{s0} = -\frac{F}{2\pi r_0 R z}, \quad r = r_0 \quad (22)$$

204 Numerical implementation

205 TELL THAT THERE IS ALSO A LINEAR SOLUTION BUT IT WONT BE
 206 SHOWN IN THE PAPER. ALSO, THAT IT WONT BE SHOWN THE SO-
 207 LUTIONS FOR THE COMPARED MODELS. CITE THE THESIS.

208 In the numerical solution, the combined water and solute movement is sim-
 209 ulated iteratively. In a first step, the water movement towards the root is sim-
 210 ulated, assuming salt concentrations from the previous time step. In a second
 211 step, the salt contents per segment are updated and new values for the osmotic
 212 head in all segments are calculated. The first step is then repeated with up-
 213 dated values for the osmotic heads. This process is repeated until the pressure
 214 head values and osmotic head values between iterations converge. Flowcharts
 215 containing the algorithm structure are shown in the Appendix ??.

216 The implicit numerical discretization of Equation 11 yields:

$$\begin{aligned} \theta_i^{j+1} C_i^{j+1} - \theta_i^j C_i^j &= \frac{\Delta t}{2r_i \Delta r_i} \times \\ &\left\{ \frac{r_{i-1/2}}{r_i - r_{i-1}} \left[q_{i-1/2} (C_{i-1}^{j+1} \Delta r_i + C_i^{j+1} \Delta r_{i-1}) - 2D_{i-1/2}^{j+1} (C_i^{j+1} - C_{i-1}^{j+1}) \right] - \right. \\ &\left. \frac{r_{i+1/2}}{r_{i+1} - r_i} \left[q_{i+1/2} (C_i^{j+1} \Delta r_{i+1} + C_{i+1}^{j+1} \Delta r_i) - 2D_{i+1/2}^{j+1} (C_{i+1}^{j+1} - C_i^{j+1}) \right] \right\} \end{aligned} \quad (23)$$

217 Applying equation 23 to each segment, the concentrations for the next time
 218 step C_i^{j+1} (mol m⁻³) are obtained by solving the following tridiagonal matrix:

$$\begin{bmatrix} b_1 & c_1 & & & & \\ a_2 & b_2 & c_2 & & & \\ & a_3 & b_3 & c_3 & & \\ & & \ddots & \ddots & \ddots & \\ & & & a_{n-1} & b_{n-1} & c_{n-1} \\ & & & & a_n & b_n \end{bmatrix} \begin{bmatrix} C_1^{j+1} \\ C_2^{j+1} \\ C_3^{j+1} \\ \vdots \\ C_{n-1}^{j+1} \\ C_n^{j+1} \end{bmatrix} = \begin{bmatrix} f_1 \\ f_2 \\ f_3 \\ \vdots \\ f_{n-1} \\ f_n \end{bmatrix} \quad (24)$$

219 with f_i (mol m⁻²) defined as

$$f_i = r_i \theta_i^j C_i^j \quad (25)$$

220 and a_i (m), b_i (m) and c_i (m) defined for the respective segments as described in
 221 the following.

222 1. The intermediate nodes ($i = 2$ to $i = n - 1$)

223 Rearrangement of Equation 23 to 24 results in the coefficients:

$$a_i = -\frac{r_{i-1/2}(2D_{i-1/2}^{j+1} + q_{i-1/2}\Delta r_i)\Delta t}{2(r_i - r_{i-1})\Delta r_i} \quad (26)$$

$$b_i = r_i\theta_i^{j+1} + \frac{\Delta t}{2\Delta r_i} \left[\frac{r_{i-1/2}}{(r_i - r_{i-1})}(2D_{i-1/2}^{j+1} - q_{i-1/2}\Delta r_{i-1}) + \frac{r_{i+1/2}}{(r_{i+1} - r_i)}(2D_{i+1/2}^{j+1} + q_{i+1/2}\Delta r_{i+1}) \right] \quad (27)$$

$$c_i = -\frac{r_{i+1/2}\Delta t}{2\Delta r_i(r_{i+1} - r_i)}(2D_{i+1/2}^{j+1} - q_{i+1/2}\Delta r_i) \quad (28)$$

224 2. The outer boundary ($i = n$)

225 Applying boundary condition of zero solute flux, the third and fourth
226 terms from the right hand side of Equation 23 are equal to zero. Thus,
227 the solute balance for this segment is written as:

$$\theta_n^{j+1}C_n^{j+1} - \theta_n^jC_n^j = \frac{\Delta t}{2r_n\Delta r_n} \times \left\{ \frac{r_{n-1/2}}{r_n - r_{n-1}} \left[\frac{q_{n-1/2}(C_{n-1}^{j+1}\Delta r_n + C_n^{j+1}\Delta r_{n-1}) -}{2D_{n-1/2}^{j+1}(C_n^{j+1} - C_{n-1}^{j+1})} \right] \right\} \quad (29)$$

228 Rearrangement of Equation 29 to 24 results in the coefficients:

$$a_n = -\frac{r_{n-1/2}(2D_{n-1/2}^{j+1} + q_{n-1/2}\Delta r_n)\Delta t}{2(r_n - r_{n-1})\Delta r_n} \quad (30)$$

$$b_n = r_n\theta_n^{j+1} + \frac{\Delta t}{2\Delta r_n} \left[\frac{r_{n-1/2}}{r_n - r_{n-1}}(2D_{n-1/2}^{j+1} + q_{n-1/2}\Delta r_{n-1}) \right] \quad (31)$$

229 3. The inner boundary ($i = 1$)

230 (a) For $C < C_{lim}$

231 Applying boundary conditions of non-linear concentration dependent
232 solute flux, the first and second term of the right-hand side of Equa-

233 tion 23 become $-\left(\frac{I_m}{2\pi r_0 R_z(K_m + C_1^{j+1})} + q_0\right)C_1^{j+1}\Delta r_1$:

$$\theta_1^{j+1}C_1^{j+1} - \theta_1^jC_1^j = \frac{\Delta t}{2r_1\Delta r_1} \times \left\{ \begin{array}{l} \frac{r_{1-1/2}}{r_1 - r_0} \left[- \left(\frac{I_m}{2\pi r_0 R z (K_m + C_1^{j+1})} + q_0 \right) \right] C_1^{j+1} \Delta r_1 - \\ \frac{r_{1+1/2}}{r_2 - r_1} \left[\frac{q_{1+1/2}(C_1^{j+1} \Delta r_2 + C_2^{j+1} \Delta r_1) -}{2D_{1+1/2}^{j+1}(C_2^{j+1} - C_1^{j+1})} \right] \end{array} \right\} \quad (32)$$

234 Rearrangement of Equation 32 to 24 results in the following coeffi-
 235 cients:

$$b_1 = r_1\theta_1^{j+1} + \frac{\Delta t}{2\Delta r_1} \left[\begin{array}{l} \frac{r_{1+1/2}}{(r_2 - r_1)} (2D_{1+1/2}^{j+1} + q_{i+1/2}\Delta r_2) + \\ \frac{r_{1-1/2}}{r_1 - r_0} \left(\frac{I_m}{2\pi r_0 R z (K_m + C_1^{j+1})} + q_0 \right) \Delta r_1 \end{array} \right] \quad (33)$$

$$c_1 = -\frac{r_{1+1/2}\Delta t}{2\Delta r_1(r_2 - r_1)} (2D_{1+1/2}^{j+1} - q_{1+1/2}\Delta r_1) \quad (34)$$

- 236 (b) For $C_{lim} < C < C_2$
 237 (c) For $C = 0$

238 References

- 239 Michael A Celia, Efthimios T Bouloutas, and Rebecca L Zarba. A general mass-
 240 conservative numerical solution for the unsaturated flow equation. *Water*
 241 *resources research*, 26(7):1483–1496, 1990.
- 242 Quirijn De Jong van Lier, Klaas Metselaar, and Jos C. Van Dam. Root wa-
 243 ter extraction and limiting soil hydraulic conditions estimated by numerical
 244 simulation. *Vadose Zone Journal*, 5(4):1264–1277, 2006.
- 245 Quirijn De Jong van Lier, Jos C. Van Dam, and Klaas Metselaar. Root water
 246 extraction under combined water and osmotic stress. *Soil Science Society of*
 247 *America Journal*, 73(3):862–875, 2009.
- 248 P.B. Tinker and P.H. Nye. *Solute Movement in the Rhizosphere*. Topics in
 249 sustainable agronomy. Oxford University Press, 2000.
- 250 Jos C Van Dam and Reinder A Feddes. Numerical simulation of infiltration,
 251 evaporation and shallow groundwater levels with the richards equation. *Jour-*
 252 *nal of Hydrology*, 233(1):72–85, 2000.
- 253 M Th Van Genuchten. A closed-form equation for predicting the hydraulic
 254 conductivity of unsaturated soils. *Soil science society of America journal*, 44
 255 (5):892–898, 1980.

256 J H M Wösten, G J Veerman, W J M De Groot, and J Stolte. Waterretentie-en
257 doorlatendheidskarakteristieken van boven-en ondergronden in nederland: de
258 staringsreeks. 2001.

259 Figures

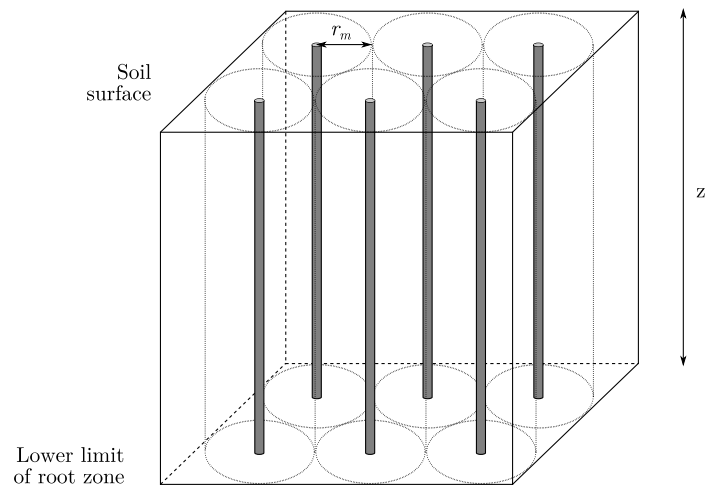


Figure 1: Schematic representation of the spatial distribution of roots in the root zone

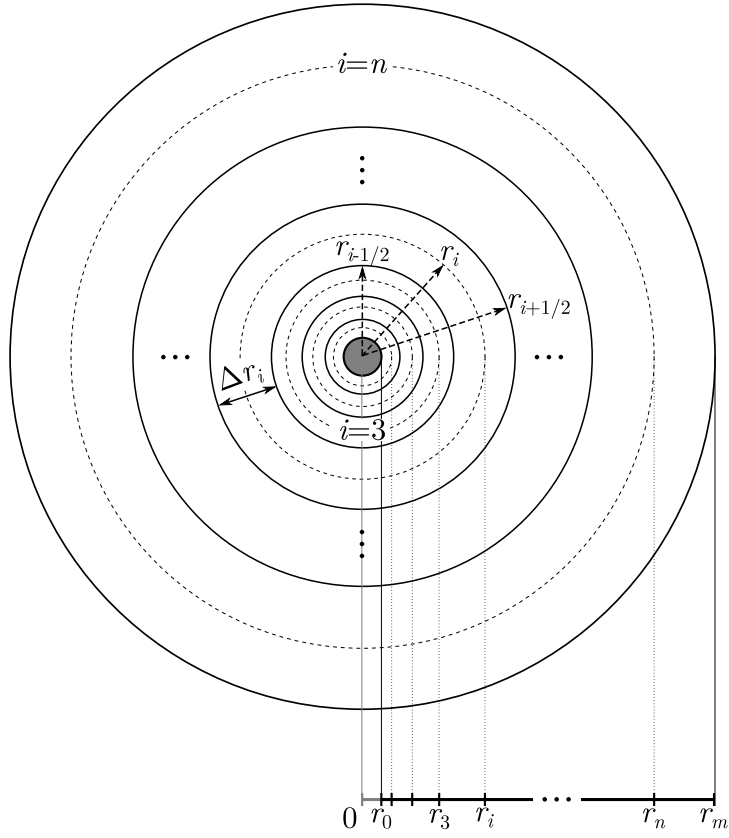


Figure 2: Schematic representation of the discretized domain considered in the model. Δr is the variable segment size, increasing with the distance from the root surface (r_0) to the half-distance between roots (r_m), and n is the number of segments

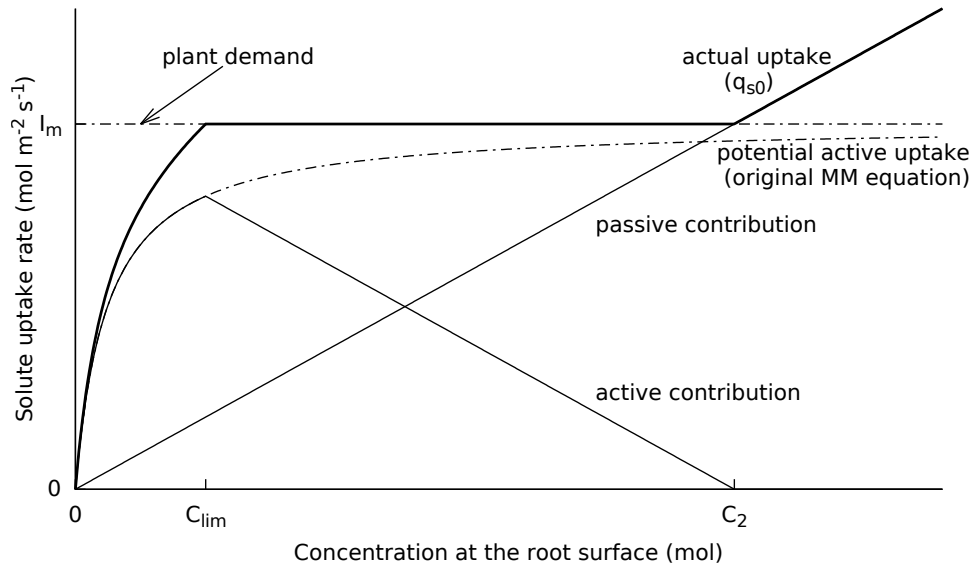


Figure 3: Solute uptake piecewise equation from MM equation 15 with boundary conditions. The bold line represents the actual uptake, thin lines represent active and passive contributions to the actual uptake, and dotted lines represent the plant demand and the potential active uptake